ACS APPLIED MATERIALS & INTERFACES

Research Article

www.acsami.org

Attogram Detection of Picric Acid by Hexa-*peri*-Hexabenzocoronene-Based Chemosensors by Controlled Aggregation-Induced Emission Enhancement

Varun Vij, Vandana Bhalla,* and Manoj Kumar*

Department of Chemistry, UGC Centre for Advanced Studies, Guru Nanak Dev University, Amritsar (Punjab), India 143005

Supporting Information

ABSTRACT: Hexa-*peri*-hexabenzocoronene (HBC) based molecules **5** and **6** have been designed and synthesized. These planar coronenes are appended with rotors to invoke aggregation induced emission enhancement (AIEE) phenomenon by controlling the ratio of H_2O in solutions of aggregates. These aggregates of HBC derivatives serve as highly selective chemosensors for picric acid (PA) in mixed aqueous solution. These aggregates are also able to detect PA in vapor phase. In addition, fluorescent test strips have been prepared by dip-coating the Whatman paper with aggregates of both compounds for trace detection of PA in contact mode with detection limits in attograms.

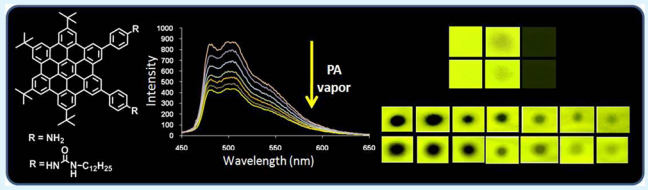

KEYWORDS: *hexa-peri-hexabenzocoronene, aggregation induced emission enhancement, picric acid, vapor phase detection, attogram detection*

INTRODUCTION

The explosive nature of picric acid (PA) has been exploited for a long time in preparation of lethal weapons like bombs, grenades, etc., and large residual amounts of PA are still likely to be deposited in anionic form as photolysis product in soil of war affected areas. These undetected traces of explosives have many adverse health effects on mammals living around.[1] In anhydrous state, PA is highly prone to react with metals to create shock sensitive explosive metal salts.[2] In addition to this, PA has many other nonmilitary roles like as a sensitizer in photographic emulsions, as a component in matches, in medicinal formulations in the treatment of diseases like malaria, trichinosis, herpes, smallpox, and antiseptics.[3] Picric acid is also used in the analytical chemistry of metals, ores, and minerals. Bouin solution is a common picric acid-containing fixative solution used for histology specimens. Therefore, the development of methods for the trace detection of PA is an area of great research interest. Fluorescence signaling is one of the first choices among various methods used for detection of nitroderivatives due to its high sensitivity and selectivity.[4,5] To date, various fluorescent chemosensors, conjugated polymers,[6−11] fluorescent nanofibres,[12−15] and nanoparticles have been developed for detection of nitroderivatives especially trinitrotoluene (TNT) and 2,4-dinitrotoluene (DNT) etc.[16−19] Though explosive power of PA is superior to that of TNT yet less attention has been paid to development of methods for selective and sensitive detection of PA. Although there are several reports on fluorogenic sensors for detection of PA[20−27] yet the majority of reports lack the combination of high selectivity and low detection limit which are the main requirements for practical utility of PA sensors. Besides, because of low vapor pressure of PA in comparison to other nitroderivatives, the vapor phase detection of PA still remains a challenge. Recently, AIEE active materials have been used as sensors for the detection of nitroaromatics.[28−30] Because aggregation-induced emission enhancement exhibiting materials offer more diffusion channels for the exciton to migrate, they are more quickly annihilated by the nitro explosives.

Recently from our lab, chemosensors for detection of picric acid have been reported.[31,32] An AIEE active thiophene-based pentaquinone derivative has been reported that exhibited moderate selectivity toward PA among other nitro derivatives with low quenching constant and low detection limit in range of μM concentration. However, no vapor phase detection of PA was discussed.[31] In another work, we used a Hg^{2+} ensemble of a derivative bearing N,N-dimethylcinnamic group for selective detection of PA with low quenching constant. This derivative also did not exhibit any PA detection in vapor or solid state.[32] To overcome these limitations, we were now interested in development of fluorescent supramolecular assemblies for selective and sensitive detection of picric acid in solution as well as vapor phase, with detection limit in range of femtograms or attograms. Hexa-*peri*-hexabenzocoronene (HBC) is the molecule of our choice to develop chemosensors for PA. HBC derivatives, because of their flat, rigid, and discotic core, have attracted long-term interest for the formation of supramolecular self-assembled columnar architectures. These self-assembled architectures render a tremendous potential in

Received: April 18, 2013
Accepted: May 21, 2013
Published: May 21, 2013

these derivatives for material applications.[33−35] The favorable overlap of π-orbitals in adjacent molecules significantly increases the charge carrier mobility which raises the potential of these molecules for fabricating electronic devices for one-dimensional energy/charge migration, electrical conductivity and photoconductivity with exceptionally high transport properties.[36−43] Adversely, these intermolecular π-interactions decrease the solubility and photolumniscence of HBC derivatives because of aggregation-caused quenching,[44−46] which reduces the potential of these fluorescent aggregates as chemosensing materials. Herein, we have designed and synthesized HBC derivatives **5** and **6**, which form fluorescent aggregates in mixed aqueous media. These derivatives possess sterically demanding *tert*-butyl groups at periphery which enhance the solubility. Further, we have introduced two rotatable phenyl groups as rotors, which render the aggregation induced emission enhancement phenomenon in coronene based molecules which can increase the utility of HBC moiety as fluorogenic chemosensor. Interestingly, derivatives **5** and **6** exhibit aggregation-induced emission enhancement and form spherical aggregates in mixed aqueous media, which behave as potential chemosensors for PA. In addition, these aggregates are able to detect the PA in vapor state. To the best of our knowledge, this is the first report on HBC exhibiting aggregation-induced emission enhancement (AIEE) phenomenon to give fluorogenic aggregates which serve as selective chemosensors for detection of PA in solution as well as vapor state. To promote convenient, economic, and highly sensitive detection of PA, we prepared the fluorescent test strips. These test strips can detect PA in vapor and contact mode up to attogram level, which can be helpful for trace detection of piric acid.

RESULTS AND DISCUSSION

The reaction of compound **1**[47] with *tert*-butylchloride in the presence of catalytic amount of $FeCl_3$ in nitromethane followed by cyclodehydrogenation in a one-pot, two-step reaction afforded HBC derivative **2** (Scheme 2). The boronic ester **4** was synthesized by the condensation reaction of compound **3**[48] with dodecylisocyanate in dry THF (Scheme 1). Further,

Scheme 1. Synthetic Scheme for Boronic Ester 4

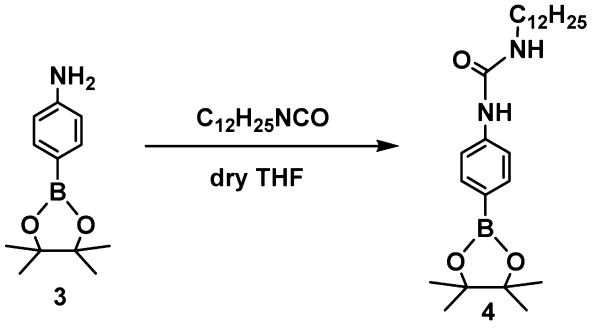

Suzuki−Miyaura cross coupling of compound **2** with aniline boronic ester **3** afforded HBC derivative **5** (Scheme 2). Under same conditions as used for the synthesis of compound **5**, derivative **6** was synthesized by Suzuki-Miyaura coupling of compound **2** with boronic ester **4** (Scheme 2). The structures of compounds **4**, **5** and **6** were confirmed from their spectroscopic and analytical data (Supporting Information, S3−S14). ^{1}H NMR of compound **2** shows three broad signals at 8.38, 8.70, and 9.00 ppm corresponding to the aromatic protons and two singlets at 1.82 and 2.04 ppm corresponding to protons of *tert*-butyl groups. ^{1}H NMR of compound **4** shows two doublets at 7.28 and 7.72 ppm corresponding to aromatic protons, two triplets at 0.87 and 1.49 ppm due to terminal CH_3 and NCH_2, respectively, one singlet at 1.25 corresponding to CH_2 groups of dodecyl chain, and two broad signals at 4.93 and 6.60 ppm due to NH protons. Further, ^{1}H NMR of compound **5** shows three broad signal at 8.51, 8.82, and 9.98 ppm due to aromatic protons, two doublets at 7.10 and 7.87 ppm due to aromatic protons, and two singlets at 1.72 and 1.88 ppm corresponding to the protons of *tert*-butyl groups. ESI-MS spectrum of derivative **5** shows parent ion peak at 929 $(M+1)^+$. ^{1}H NMR of compound **6** shows three broad signal at 8.58, 8.79, and 9.21 ppm due to aromatic protons, two doublets at 7.75 and 7.92 ppm due to aromatic protons, and two singlets at 1.74 and 1.85 ppm corresponding to protons of *tert*-butyl groups,two broad signals at 1.29 and 3.40 ppm due to CH_2 groups of alkyl chains, one triplet at 0.89 ppm due to terminal CH_3 protons, and two broad signals at 5.12 and 5.91 ppm due to NH protons. ESI-MS spectrum of derivative **6** shows parent ion peak at 1351.60 (M^+). These spectroscopic data corroborates with the structures **2**, **4**, **5**, and **6** for these compounds.

The UV−vis spectrum of compound **5** shows absorption band at 368 and 398 nm in THF. However, the increase of H_2O fraction in THF solution up to 40% leads to the increase in these bands along with the formation of leveling off tail which is due to the formation of nanoaggregates in solution (Supporting Information, Figure S1).[49] In fluorescence spectrum, compound **5** (1 μM) exhibits emission band (ϕ_0 = 0.41)[50] at 485 and 510 nm in pure THF when excited at 368 nm. The subsequent increase in % age of H_2O fraction up to 40% leads to the 67% enhancement of emission (ϕ_{AIEE} = 0.68) (Figure 1). This increase in fluorescence intensity can be attributed to the aggregation induced emission enhancement (AIEE) caused by the restriction in rotation of otherwise freely rotatable substituted phenyl groups (rotors). However, a further increase in water content in the solution leads to the decrease in the emission intensity (ϕ_{ACQ} = 0.09) along with slight red shift of 13 nm (Figure 1). This is probably due to $\pi-\pi$ interactions between coronene cores, which reduce the intramolecular π-conjugation, thus decreasing the emission intensity. In case of HBC derivative **6**, with increase in ratio of H_2O up to 40% in THF, the absorption band at 370 nm corresponding to derivative **6** increases with appearance of leveling off tail in visible region (see the Supporting Information, Figure S2). In fluorescence spectrum, HBC derivative **6** exhibits 86% emission enhancement (ϕ_{AIEE} = 0.73) in H_2O:THF (4:6) in comparison to the solution in pure THF (ϕ_0 = 0.47) (see the Supporting Information, Figure S3). Therefore in these molecules, aggregation-induced emission enhancement can be controlled by restricting ratio of H_2O in the solution of aggregates.

The formation of aggregates was further confirmed by the scanning electron microscopic (SEM) images of derivatives **5** and **6** which show the formation of spherical aggregates of average size of 200 and 150 nm in H_2O:THF (4:6) (Figure 2a, b), respectively. Interestingly, the water content in the solution of aggregates of derivatives **5** and **6** increases up to 90% H_2O, which confirms the formation of wire-shaped assembly (Figure 2c, d, respectively), possibly due to $\pi-\pi$ intermolecular interactions between discotic molecules. We envisioned that if this mechanism is indeed at work, the solution of compounds **5**

Scheme 2. Synthetic Scheme for Hexa-*peri*-hexabenzocoronene-Based Derivatives 5 and 6[a]

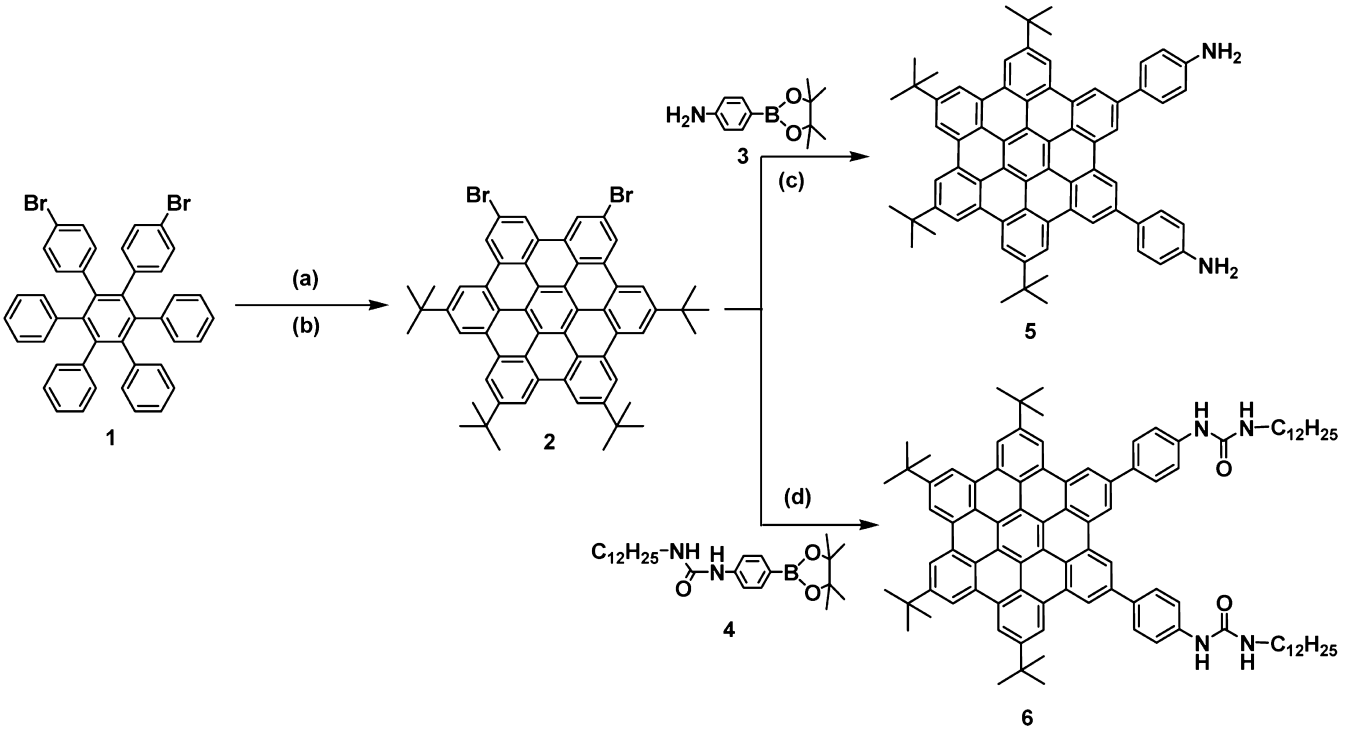

[a](a) *Tert*-butylchloride, $FeCl_3$, and $MeNO_2$, RT; (b) $FeCl_3$ and $MeNO_2$, RT; (c, d) THF, K_2CO_3, $PdCl_2(PPh_3)_2$, H_2O, under N_2, reflux.

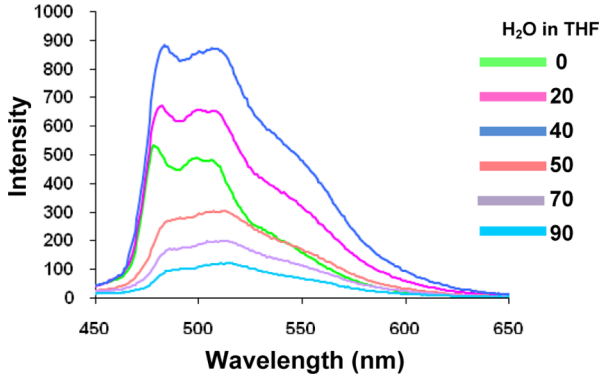

Figure 1. Fluorescence spectrum of compound **5** (1 μM) in different H_2O:THF ratios at 3:5 slit width.

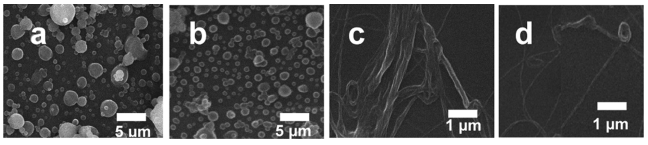

Figure 2. Scanning electron microscope images of derivatives **5** and **6** in (a, b) H_2O:THF, 4:6 and (c, d) H_2O:THF, 9:1, respectively.

and **6** should become more emissive with increase in viscosity as thickening process is known to hamper intramolecular rotations.[51] To confirm the mechanism of aggregation-induced emission enhancement, we recorded the fluorescence spectra of derivatives **5** and **6** in highly viscous glycerol. The spectra show much higher emission than that in the THF (see the Supporting Information, Figure S4), thus confirming the AIEE mechanism. Further, the concentration-dependent emission studies of compounds **5** and **6** in THF exhibit nonlinear increase in emission intensity with increase in concentration (see the Supporting Information, Figures S5 and S6) up to 1 μM, which supports that emission enhancement is due to aggregation mechanism instead of normal concentration-dependent emission and thus proves the mechanism.

Further, to investigate the properties of **5** and **6** as AIEE active materials for recognition of nitroaromatics, we studied the fluorescence behavior of **5** and **6** toward different nitro compounds viz. picric acid (PA), 2,4,6-trinitrotoluene (TNT), 2,4-dinitrotoluene (DNT), 1,4-dintrobenzene (DNB), *p*-nitrotoluene (PNT), *p*-nitrobenzene (PNB), 2,3-dinitro-2,3-dimethyl butane (DNDMB), and a reference aromatic compound benzoquinone (BQ).

It was observed that on addition of 5 μM of PA to the solution of **5** in 4:6 H_2O:THF, 98% quenching of fluorescence emission was observed (Figure 3). The quenching in fluorescence of compound **5** (H_2O:THF, 4:6) on the addition of PA can also be observed by the naked eye (Inset, Figure 3).

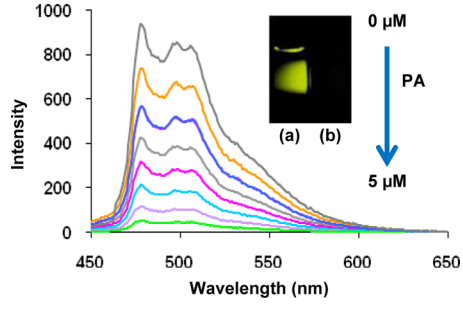

Figure 3. Fluorescence spectrum of compound **5** (1 μM) on addition of PA in 4:6 H_2O:THF. Inset shows the quenching in fluorescence of **5** after addition of PA. All images are taken under 365 nm UV lamp.

dx.doi.org/10.1021/am401414g | *ACS Appl. Mater. Interfaces* 2013, 5, 5373−5380

The Stern–Volmer plot of aggregates of **5** is linear (Figure 4) with high quenching constant K_{SV} of 3.2 × 10^6 M^{-1}. In the

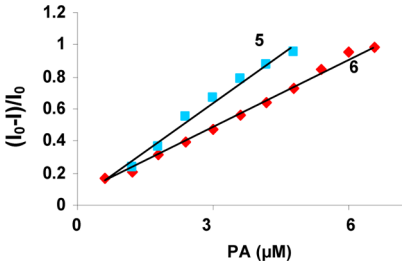

Figure 4. Stern–Volmer plot of quenching of aggregates of derivatives **5** and **6** with PA.

UV–vis spectrum, the subsequent addition of PA to the solution of aggregates of derivative **5** results in an increase in absorption band at 368 nm, which indicates the interaction between aggregates of derivatives **5** with PA (see the Supporting Information, Figure S7). We propose that the quenching of fluorescence of aggregates of **5** on addition of nitroaromatics is ascribed to the static quenching. The picric acid, being a strong acid, has a great tendency to transfer proton from its hydroxyl group to the basic amino group to make electrostatic complex between host and guest (Scheme 3). This strong complexation between compound **5** and PA facilitates the electron transfer from the photoexcited HBC to the electron deficient PA so as to shift the electron to nonradiating decay path and quench the fluorescence emission.

To verify the quenching mechanism, we analyzed the effect of pH (3–8) on quenching efficiency using universal buffer. At pH 2, 4 and 6, the derivative **5** exhibits 20, 35, and 75% quenching, respectively, on subsequent addition of 5 μM of PA to each solution. Thus, the decrease in pH value results in dramatic decrease in % quenching in emission of aggregates of **5** on addition of equivalent amount of PA (5 μM) in comparison to the % quenching (96%) at neutral pH 7. At low pH, the electrostatic interactions between complex and picric acid are weakened because of already protonated NH_2 groups. As a result, the electrostatic interactions between aggregates of **5** and PA are inhibited and electron transfer from HBC to picric acid is constrained. However, slight decrease in % quenching (90%) was observed at higher pH 8 (see the Supporting Information, Figure S8).

To confirm the mechanism of fluorescence quenching of derivative **5** in aggregated state, we carried out the ^{1}H NMR studies of aggregates of **5** (in 4:6, D_2O:THF-d_8) in the presence of PA, which show a downfield shift of 0.37 ppm in the signal of protons (from 5.25 to 5.62 ppm) of NH_2 groups (see the Supporting Information, Figure S9). This downfield shift is due to the protonation of the nitrogen atom of the NH_2 groups by PA, which is the only plausible site for protonation, thus leading to the deshielding of the protons. This ionic interactions between host and guest molecules assist the electron transfer from photoexcited HBC core to the electron deficient PA, hence resulting into quenching of emission intensity.

Under same set of conditions, derivative **6** exhibits 96% quenching on addition of 10 μM of PA (see the Supporting Information, Figure S10). The aggregates of derivative **6** also exhibits linear Stern–Volmer plot (Figure 4) with K_{SV} of 2.0 × 10^6 M^{-1}. In UV–vis spectra, the absorption band at 370 nm increases with subsequent addition of PA, which indicates the interactions between aggregates of derivative **6** and PA (see the Supporting Information, Figure S11). In the case of HBC derivative **6**, no significant effect was observed on quenching efficiency at acidic or basic pH which discards the possibility of ionic mechanism and favors the intermolecular charge transfer mechanism (see the Supporting Information, Figure S8). However in ^{1}H NMR of aggregates of derivative **6**, no significant shift in protons of NH groups of urea was observed (see the Supporting Information, Figure S12) which implies that protonation of weakly basic NH groups of urea moieties is inhibited in case of HBC derivative **6**. Therefore, the main quenching mechanism is probably the charge transfer from LUMO of photoexcited HBC unit to LUMO of PA (−3.8 eV).[52] Because of stronger ionic interactions of PA with derivative **5** in comparison to with derivative **6**, the former exhibits better quenching behavior with lower detection limit and greater Stern–Volmer constants. The aggregates of derivatives **5** and **6** possess detection limits of 4 nM and 9

Scheme 3. Quenching Mechanism of Aggregates of Derivative 5 with PA

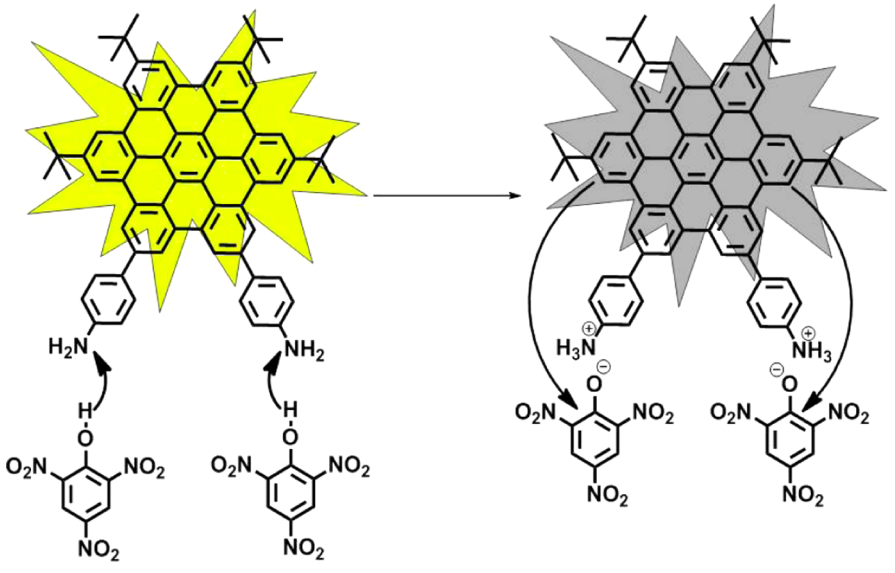

dx.doi.org/10.1021/am401414g | ACS Appl. Mater. Interfaces 2013, 5, 5373–5380

nM, respectively, as fluorescent sensors for PA (see the Supporting Information, Figure S13).

Because the absorption band of picric acid lies within the region of absorption maxima of derivatives **5** and **6**, the quenching in emission intensities can be attributed to the absorption of the excitation energy by PA instead of by respective aggregates. Thus, we carried out the fluorescence titrations of derivatives **5** and **6** with addition of equivalent amounts of PA at various excitation wavelengths (300, 310, 320, 330, 340, 350, 360, 370, 380, 390, and 400 nm). Though the fluorescence intensities of derivatives **5**/**6** at different excitation wavelengths are different, the % quenching by PA is same at all excitation wavelengths (see the Supporting Information, Figure S14). These results ruled out the possibility of decrease in fluorescence intensities of aggregates of **5** and **6** due to masking by PA.

We also studied the response of other nitro derivatives such as DNB, TNT, DNT, *p*-NT, NB, DNDMB, and BQ on the fluorescence emission of aggregates of derivatives **5** and **6**. No significant change in its fluorescence emission was observed on addition of equivalent amount of other nitroderivatives and benzoquinone (Figure 5). Because of a lack of tendency to

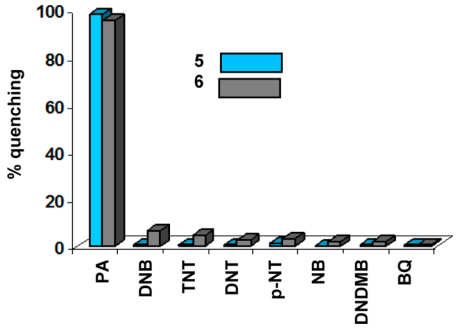

Figure 5. Selectivity graph of aggregates of derivatives **5** and **6** toward PA.

protonate the NH_2 groups of derivative **5**, other nitro derivatives do not follow ionic mechanism which reduces the quenching efficiencies of these nitro derivatives in comparison to PA. On the other hand, the selectivity of derivative **6** toward PA can be attributed to the high polarizability of PA in comparison to other nitro derivatives.[17,53]

In addition to this, the normalized overlay of absorption spectrum of PA and emission spectra of **5** and **6** do not show a significant overlap (see the Supporting Information, Figure S15) which rules out the energy transfer as the quenching mechanism for PA in both cases. The charge transfer mechanism was further confirmed by the cyclic voltammetry. The higher energy of LUMOs (lowest unoccupied molecular orbital) of **5** (−3.4 eV) and **6** (−3.3 eV) facilitates the electron to jump to the lower energy LUMO of PA (−3.8 eV) (see the Supporting Information, Figure S16).

Because derivative **5** follows ionic mechanism for quenching with PA, we studied the fluorogenic effects of anions on the quenching process by adding various anions (100 μM) to the **5-PA** ionic complex. No considerable change was observed in case of all anions which raise the practical applicability of derivative **5** toward PA sensing (see the Supporting Information, Figure S17).

Further, we studied the sensing behavior of adductive compound **5-PA** toward 2-ethylhexylamine by its subsequent addition (30 μM in H_2O/THF (4:6)) to the solution of **5-PA** in H_2O:THF (4:6) which results in revival of emission of derivative **5** (see the Supporting Information, Figure S18). This revival of emission may be attributed to higher tendency of PA to protonate NH_2 group of 2-ethylhexaylamine in comparison to derivative **5**. This study can provide a new platform for chemosensing of various competitive amines using nitro derivative adducts.

For detection of PA vapors, we exposed solution of aggregates of **5** and **6** in H_2O:THF (4:6) to vapors of PA by inserting the vial containing solution into a sealed vial containing solid PA at room temperature after every five minutes. The 34% and 21% quenching of **5** (inset, Figure 6)

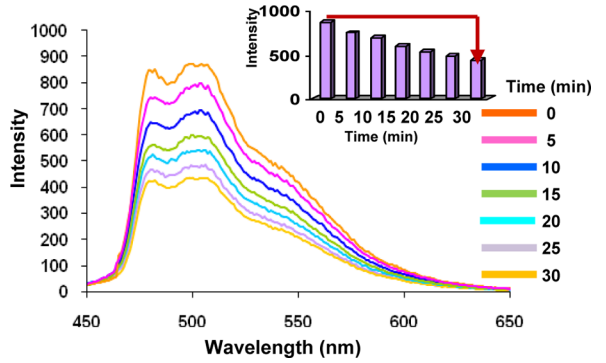

Figure 6. Change in fluorescence spectrum of derivative **5** on exposure to vapors of PA after different time intervals. Inset shows change in emission intensity of derivative **5** on exposure to PA with time.

and **6** (see the Supporting Information, Figure S19) solution in H_2O:THF (4:6) is observed, respectively, within 5 min, which went up to 64% (Figure 6) and 57% (see the Supporting Information, S19) quenching of emission intensity after 30 min, respectively, at room temperature. These results reveal that aggregates of **5** and **6** are responsive to PA in solution and vapor phase. Thus, these HBC derivatives **5** and **6** behave as better PA sensor than many previous sensors reported in terms of selectivity, sensitivity and ease of vapor phase detection (see the Supporting Information, Table S1).

Further, during preparation and usage of nitroaromatics, the human body and other materials in the surroundings are contaminated with trace amounts of explosives.[54,55] Detection of these traces and vapors of nitro explosives are major concern in the field of analytical and forensic sciences. In this context, we prepared test strips by dip-coating solutions of aggregates of **5** and **6** in H_2O:THF (4:6) on Whatman filter paper followed by drying the strips under vacuum to test the residual contamination in contact and vapor modes. Thus, we performed the paper strip test of both derivatives in vapor mode and contact mode (Figure 7). To signify the vapor mode test, we performed a paper strip test in vapor mode by placing fluorescent paper strips over the top of the glass vial containing solid PA for 15 min at room temperature. The circular area that was exposed to the PA vapors was quenched (Figure 7A (b and f)). To check the reversibility of test strip, we washed it with ethanol, which results in the revival of emission intensity attributing to the removal of the PA from test strip (Figure 7A (c and g)). The fluorescence spectra of the quenched areas of test strips of derivative **5** (Figure 8) and **6** (see the Supporting Information, Figure S20) were recorded using front face technique and compared with the emission of respective virgin

dx.doi.org/10.1021/am401414g | ACS Appl. Mater. Interfaces 2013, 5, 5373−5380

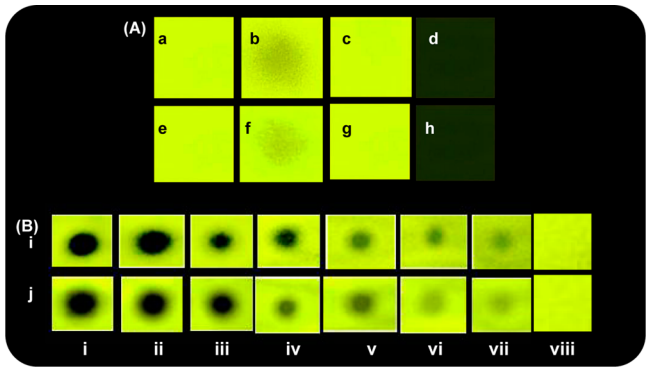

Figure 7. (A) (a, e) Virgin test strips and (d, h) after dipping the test strip of **5** and **6**, respectively, in the PA solution (1×10^{-5} M in THF). (b, f) Quenching in fluorescence of area exposed to the vapors of PA. (B) By applying a small spot of different concentrations of PA ((i) 2×10^{-3} M, (ii) 1×10^{-4} M, (iii) 1×10^{-6} M, (iv) 1×10^{-8} M, (v) 1×10^{-10} M, (vi) 1×10^{-12} M, (vii) 1×10^{-14} M, and (viii) blank solvent (THF) on test strips made from aggregates of (i) **5** and (j) **6**.

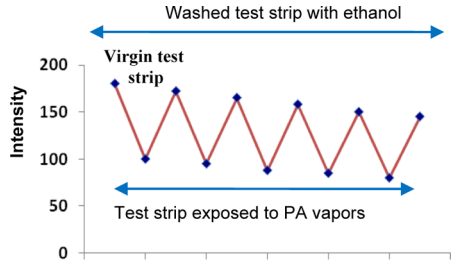

Figure 8. Reversibility experiment of fluorescent paper strip of derivative **5** for vapor phase detection of PA by washing with ethanol.

test strips, which shows 45 and 35% fluorescence quenching, respectively. The revival of fluorescence emission of test strips on washing with ethanol was also observed in fluorescence spectra of test strips. These experiments were repeated several times, which indicate the reusability of these test strips for detection of vapors of PA.

In contact mode detection, the quenching in emission was observed upon dipping the test strips of **5** and **6** into the solution of PA (1×10^{-5} M) (Figure 7A (d and h)). We also checked the effect of various concentrations of PA solution on the fluorescent paper strip by applying small spots of different concentrations of PA (10 μL) on test strips. Dark spots of different strengths can be observed which show the regulation of the quenching behavior of PA (Figure 7Bi–vii), which is also practically applicable by varying the concentration of PA even up to 10 femtomolar, i.e., 23 $\times 10^{-18}$ gram (23 attogram) (Figure 7B vii).[6a] However, no visible change was observed by applying blank solvent (THF) over the fluorescent paper strips (Figure 7Bviii).

The emission spectra of quenched area on the fluorescent test strips of derivatives **5** (Figure 9) and **6** (see the Supporting Information, Figure S21) were recorded using front face technique after applying the spots of PA (10 μL) of varying concentration (2×10^{-3}, 1×10^{-4}, 1×10^{-6}, 1×10^{-8}, 1×10^{-10}, 1×10^{-12}, 1×10^{-14} M) (Figure 9). The emission spectra of test strips of derivatives **5** and **6** exhibit 45 and 40% quenching, respectively, with 10^{-14} M solution of PA. However, no effect of blank solvent was observed on the emission intensity of fluorescent paper strips of derivatives **5** (Figure 9) and **6** (see the Supporting Information, Figure S21). These

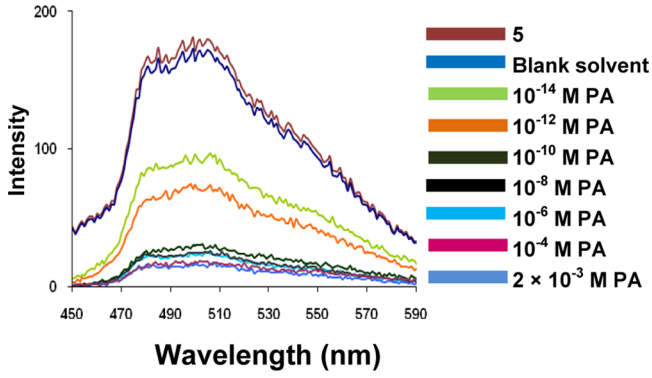

Figure 9. Fluorescence spectra of dip-coated paper strips of aggregates of **5** (1 μM) after applying spot of PA (10 μL) using front face fluorescence method at λ_{ex} = 368 nm.

results show the practical applicability of both derivatives **5** and **6** toward instant and economical detection of traces of PA up to attogram level by naked eye. The nanoaggregates of **5** and **6** favors long-range exciton diffusion. Thus, the fast excitation energy diffusion within the aggregates and between the aggregates facilitates efficient electron/charge transfer mechanisms to be annihilated by low amount of the picric acid, resulting in attogram level detection. Thus, fluorescent test strips exhibit very high sensitivity toward PA.

CONCLUSION

We designed and synthesized two HBC based derivatives **5** and **6** incorporated with two rotors which induce controlled AIEE by restricting the ratio of water in solution of aggregates. The aggregates of both derivatives behave as highly sensitive and selective chemosensor for picric acid. We have also compared the potential of both chemosensors based on the quenching mechanism followed by them depending upon the functional groups attached to the central coronene ring. Both derivatives show very low detection limit and very high Stern–Volmer constants, which is major requirement for practical usage of chemosensors. Besides, both chemosensors exhibit efficient quenching in emission on exposure to the vapors of picric acid at room temperature which enhances the practical application of these chemosensors. In addition to this, we have prepared the fluorescent test strips carrying aggregates of derivatives **5** and **6**, which can detect the PA up to attogram level.

EXPERIMENTAL SECTION

General Information. All the fluorescence spectra were recorded on SHIMADZU 5301 PC spectrofluorimeter. The emission spectra of fluorescent test strips were recorded by front face technique on SHIMADZU 5301 PC spectrofluorimeter. UV spectra were recorded on Shimadzu UV-2450PC spectrophotometer with a quartz cuvette (path length: 1 cm). The cell holder was thermostatted at 25 °C. Elemental analysis was done using Flash EA 1112 CHNS/O analyzer of Thermo Electron Corporation. ^{1}H and ^{13}C NMR spectra were recorded on JEOL-FT NMR-AL 300 MHz and Bruker (Avance II) FT-NMR 400 MHz spectrophotometer using $CDCl_3$, D_2O and THF-d_8 as solvent and TMS as internal standards. Data are reported as follows: chemical shifts in parts per million (δ), multiplicity (br = broad signal, s = singlet, d = doublet, t = triplet, m = multiplet), coupling constants (Hz), integration, and interpretation. Silica Gel 60 (60–120 mesh) was used for column chromatography.

Experimental Details of Preparation of Fluorescent Test Strips. The fluorescent test strips were prepared by dip coating of

Whatman filter paper (6 cm × 6 cm) in the solution of aggregates of **5**/**6** in H_2O/THF (4:6) followed by drying these strips in vacuum.

Experimental Details of Vapor Phase Detection of Picric Acid. A glass vial containing 3 mL of a bsolution of aggregates of derivative **5**/**6** was inserted in a bigger glass vial containing crystals of picric acid. The system was sealed tightly to saturate the system with vapors of PA at room temperature. The fluorescent spectra of this solution were recorded after every 5 min of keeping it in saturated vapors of PA in a closed system.

For vapor phase detection of PA by fluorescent paper strips, we kept the paper strip over the mouth of the vial containing crystals of PA for 15 min. The area exposed to the vapors of PA exhibits quenching in fluorescence visible to naked eye.

Experimental Details of Finding Detection Limit. To determine the detection limits, the fluorescence titrations of 1×10^{-7} M solution of compounds **5** and **6** with PA were carried out by adding aliquots of PA solution of micromolar concentration and the fluorescence intensity as a function of PA added was then plotted. From this graph the concentration at which there was a sharp change in the fluorescence intensity multiplied with the concentration of receptors **5** and **6** gave the detection limits.

Syntheses. Compounds **1**[47] and **3**[48] were synthesized according to the literature procedures.

Synthesis of Compound ***2***. To the nitrogen sparged solution of compound **1** (0.5 g, 0.72 mmol) in dichloromethane was added *tert*-butylchloride (0.397 g, 4.32 mmol), followed by the addition of $FeCl_3$ (5.8 mg, 0.36 mmol) solution in nitromethane (0.5 mL). The reaction mixture was sparged with nitrogen and stirred at room temperature for 30 min. After 30 min, a solution of $FeCl_3$ (2.8 g, 17.28 mmol) in 3 mL of nitromethane was added and stirred for 2 h. The reaction mixture was poured into methanol (100 mL) and the precipitates were filtered and washed with methanol to afford compound **2**, which was further purified by column chromatography using $CHCl_3$ as eluent to yield compound **2** in 53% yield. Mp > 250 °C. ^{1}H NMR (300 MHz, $CDCl_3$): δ (ppm) 1.83 (s, 18H, $C(CH_3)_3$), 2.04 (s, 18H, $C(CH_3)_3$), 8.38 (br, 4H, ArH), 8.70 (br, 4H, ArH), 9.00 (br, 4H, ArH). ^{13}C NMR (75 MHz, $CDCl_3$): δ (ppm) 29.85, 30.17, 31.39, 118.13, 118.37, 118.94, 119.89, 120.90, 123.18, 124.22, 126.23, 127.97, 128.21, 129.27, 130.24, 130.97, 137.55, 137.78, 139.83, 141.36, 146.64, 151.93 ESI-MS: 904.1 (M^+). Anal. Calcd for $C_{58}H_{48}Br_2$: C, 76.99; H, 5.35; Br, 17.66. Found: C, 76.87; H, 5.30.

Synthesis of Compound ***4***. To the solution of compound **3** (0.5 g, 2.3 mmol) in dry tetrahydrofurane (6 mL) was added dodecylisocyanate (1 g, 4.6 mmol) followed by the stirring overnight at room temperature. The reaction mixture was concentrated under the reduced pressure and methanol was added. The solid precipitates were filtered and recrystallized in $CHCl_3$:methanol to afford an off-white compound **4** in 91% yield. ^{1}H NMR (300 MHz, $CDCl_3$) δ (ppm) = 0.877 (t, J = 6.0 Hz, 3H, $-CH_3$), 1.25 (s, 20H, $-CH_2$), 1.33(m, 12H, $-CH_3$), 1.49 (t, 2H, $-CH_2-$), 4.93 (br, 1H, $-$NH), 6.6 (br, 1H, $-$NH), 7.28 (d, J = 9 Hz, 2H, ArH), 7.72 (d, J = 9 Hz, 2H, ArH). ^{13}C NMR (100 MHz, DMSO-d_6): δ (ppm) 14.12, 22.67, 24.82, 26.90, 29.34, 29.62, 30.05, 31.89, 40.37, 83.62, 118.91, 135.98, 141.61, 155.76. m/z 431.3414 ($M+H^+$). Elemental anal. Calcd % for $C_{25}H_{43}BN_2O_3$: C, 69.76; H, 10.07; B, 2.51; N, 6.51; O, 11.15; Found C, 69.11; H, 10.17; N, 6.29.

Synthesis of Compound ***5***. To a solution of **2** (0.1 g, 0.11 mmol) and **3** (0.06 g, 0.28 mmol) in THF were added K_2CO_3 (0.06 mg, 0.44 mmol), distilled H_2O (1 mL), and $[Pd(Cl)_2(PPh_3)_2]$ (0.04 g, 0.055 mmol) under nitrogen and the reaction mixture was refluxed overnight. The THF was then removed under vacuum and the residue so obtained was treated with water, extracted with dichloromethane, and dried over anhydrous Na_2SO_4. The organic layer was evaporated and the compound was purified by column chromatography using chloroform as an eluent to give of compound **6**, which was further recrystallized from methanol to provide 0.054 g of white solid (yield 50%). Mp >250 °C. ^{1}H NMR (300 MHz, $CDCl_3$): δ (ppm) 1.72 (s, 18H, $C(CH_3)_3$), 1.88 (s, 18H, $C(CH_3)_3$), 7.10 (d, J = 6 Hz, 4H, ArH), 7.87 (d, J = 6 Hz, 4H, ArH) 8.51 (br, 4H, ArH), 8.82 (br, 4H, ArH), 9.08 (br, 4H, ArH) ; ^{13}C NMR (100 MHz, $CDCl_3$): δ (ppm) 29.37, 29.70, 30.09, 31.99, 32.00, 82.74, 84.52, 88.95, 97.12, 118.42, 118.65, 119.70, 122.18, 124.90, 126.89, 127.89, 128.09, 128.58, 128.54, 132.97, 133.27, 135.54, 137.76, 139.01, 141.47, 141.96, 151.15, 159.31. ESI-MS: 928.1312 $(M)^+$, 929.1199 $(M+1)^+$ and 930.1233 $(M+2)^+$. Anal. Calcd for $C_{70}H_{60}N_2$: C, 90.48; H, 6.51; N, 3.01. Found: C, 90.42; H, 6.46; N, 2.91.

Synthesis of Compound ***6***. To a solution of **2** (0.1 g, 0.11 mmol) and **4** (0.12 g, 0.28 mmol) in THF were added K_2CO_3 (0.060 mg, 0.44 mmol), distilled H_2O (3 mL), and $[Pd(Cl)_2(PPh_3)_2]$ (0.04 g, 0.055 mmol) under nitrogen and the reaction mixture was refluxed overnight. The THF was then removed under vacuum and the residue so obtained was treated with water, extracted with dichloromethane, and dried over anhydrous Na_2SO_4. The organic layer was evaporated and the compound was purified by column chromatography using chloroform as an eluent to give of compound **6** which was further recrystallized from methanol to provide 0.067 g of white solid (yield 45%). Mp >250 °C. ^{1}H NMR (300 MHz, $CDCl_3$): δ (ppm) 0.89 (t, J = 6 Hz, 6H, CH_3), 1.29 (br, 20H, CH_2), 1.74 (s, 18H, $C(CH_3)_3$), 1.85 (s, 18H, $C(CH_3)_3$), 3.40 (br, 4H, CH_2), 3.74 (), 5.12 (br, 2H, NH), 5.91 (br, 2H, NH), 7.75 (d, J = 12 Hz, 4H, ArH), 7.92 (d, J = 12 Hz, 4H, ArH) 8.58 (br, 4H, ArH), 8.79 (br, 4H, ArH), 9.21 (br, 4H, ArH). ^{13}C NMR (100 MHz, $CDCl_3$): δ (ppm) 14.11, 22.68, 27.08, 29.35, 29.68, 31.91, 39.85, 40.05, 40.26, 82.89, 84.02, 87.83, 95.84, 118.40, 119.16, 119.90, 121.86, 123.33, 126.42, 126.64, 127.15, 127.65, 128.38, 128.68, 128.76, 130.24, 132.18, 132.58, 137.15, 138.64, 147.49, 148.36, 148.64, 162.40, 171.17. ESI-MS: 1351.60 $(M)^+$. Anal. Calcd for $C_{96}H_{110}N_4O_2$: C, 85.29; H, 8.20; N, 4.14; O, 2.37 Found: C, 85.22; H, 8.02; N, 2.27.

■ ASSOCIATED CONTENT

Ⓢ Supporting Information

^{1}H, ^{13}C, mass spectra of compounds **2**,**4**, **5**, and **6**; UV−vis and fluorescence studies; detection limits; cyclic voltammograms of **5** and **6**; and table of comparison of present manuscript with previous reports. This material is available free of charge via the Internet at http://pubs.acs.org.

■ AUTHOR INFORMATION

Corresponding Author

*E-mail: mksharmaa@yahoo.co.in (M.K.); vanmanan@yahoo.co.in (V.B.).

Notes

The authors declare no competing financial interest.

■ ACKNOWLEDGMENTS

We are grateful to the DST for financial support (ref no. SR/S1/OC-69/2012 and UGC (New Delhi, India) for 'University with Potential for Excellence' (UPE) project).

■ REFERENCES

(1) Wyman, J. F.; Serve, M. P.; Hobson, D. W.; Lee, L. H.; Uddin, D. E. *J. Toxicol. Environ. Health, Part A* **1992**, *37*, 313−327.

(2) Holdsworth, G.; Johnson, M. S. *USACHPPM* **2005**, *37-EJ1138−01J*, 1−14.

(3) *Patty's Toxicology*; John Wiley & Sons: New York, 2000; Vol. *IIB*, p 980.

(4) Jian, C.; Seit, W. J. *Anal. Chim. Acta* **1990**, *237*, 265−271.

(5) Yang, X.; Niu, C. J.; Shen, G. L.; Yu, R. Q. *Analyst* **2001**, *126*, 349−352.

(6) Apodaca, D. C.; Pernites, R. B.; Mundo, F. R. D.; Advincula, R. C. *Langmuir* **2011**, *27*, 6768−6779.

(7) Thomas, S. W.; Joly, G. D.; Swager, T. M. *Chem. Rev.* **2007**, *107*, 1339−1386.

(8) Narayanan, A.; Varnavski, O. P.; Swager, T. M.; Goodson, T. *J. Phys. Chem. C* **2008**, *112*, 881−884.

(9) Che, Y.; Yang, X.; Liu, G.; Yu, C.; Ji, H.; Zuo, J.; Zhao, J.; Zang, L. *J. Am. Chem. Soc.* **2010**, *132*, 5743−5750.

(10) Wang, X.; Guo, Y.; Li, D.; Chen, H.; Sun, R.-c. *Chem. Commun.* **2012**, *48*, 5569−5571.
(11) Sanchez, J. C.; Trogler, W. C. *J. Mater. Chem.* **2008**, *18*, 3143−3156.
(12) Kartha, K. K.; Babu, S. S.; Srinivasan, S.; Ajayaghosh, A. *J. Am. Chem. Soc.* **2012**, *134*, 4834−4841.
(13) Naddo, T.; Che, Y.; Zang, W.; Balakrishnan, K.; Yang, X.; Yen, M.; Zhao, J.; Moore, J. S.; Zhang, L. *J. Am. Chem. Soc.* **2007**, *129*, 6978−6979.
(14) Zang, L.; Che, Y.; Moore, J. S. *Acc. Chem. Res.* **2008**, *41*, 1596−1608.
(15) Zhang, C.; Che, Y.; Yang, X.; Bunes, B. R.; Zang, L. *Chem. Commun.* **2010**, *46*, 5560−5562.
(16) Liu, X.; Xu, Y.; Jiang, D. *J. Am. Chem. Soc.* **2012**, *134*, 8738−8741.
(17) Venkatramaiah, N.; Kumar, S.; Patil, S. *Chem. Commun.* **2012**, *48*, 5007−5009.
(18) Shanmugaraju, S.; Joshi, S. A.; Mukherjee, P. S. *J. Mater. Chem.* **2011**, *21*, 9130−9138.
(19) Gole, B.; Shanmugaraju, S.; Bar, A. K.; Mukherjee, P. S. *Chem. Commun.* **2011**, *47*, 10046−10048.
(20) Toal, S. J.; Trogler, W. C. *J. Mater. Chem.* **2006**, *16*, 2871−2883.
(21) Li, D.; Liu, J.; Kwok, R. T. K.; Liang, Z.; Tang, B. Z.; Yu, J. *Chem. Commun.* **2012**, *48*, 7167−7169.
(22) Ding, L.; Liu, Y.; Cao, Y.; Wang, L.; Xin, Y.; Fang, Y. *J. Mater. Chem.* **2012**, *22*, 11574−11582.
(23) Shanmugaraju, S.; Jadhav, H.; Patil, Y. P.; Mukherjee, P. S. *Inorg. Chem.* **2012**, *51*, 13072−13074.
(24) Xu, Y.; Li, B.; Li, W.; Zhao, J.; Sun, S.; Pang, Y. *Chem. Commun.* **2013**, DOI: 10.1039/C3CC41994K.
(25) Liu, T.; Ding, L.; He, G.; Yang, Y.; Wang, W.; Fang, Y. *ACS Appl. Mater. Interfaces* **2011**, *3*, 1245−1253.
(26) He, G.; Peng, H.; Liu, T.; Yang, M.; Zhang, Y.; Fang, Y. *J. Mater. Chem.* **2009**, *19*, 7347−7353.
(27) Du, H.; He, G.; Liu, T.; Ding, L.; Fang, Y. *J. Photochem. Photobiol., A* **2011**, *217*, 356−362.
(28) Wang, J.; Mei, J.; Yuan, W.; Lu, P.; Qin, A.; Sun, J.; Ma, Y.; Tang, B. Z. *J. Mater. Chem.* **2011**, *21*, 4056−4059.
(29) Liu, J.; Zhing, Y.; Lu, P.; Hong, Y.; Lam, J. W. Y.; Faisal, M.; Yu, Y.; Wong, K. S.; Tang, B. Z. *Polym. Chem.* **2010**, *1*, 426−429.
(30) Lu, P.; Lam, J. W. Y.; Jim, C. K. W.; Yuan, W.; Xie, N.; Zhong, Y.; Hu, Q.; Wong, K. S.; Cheuk, K. K. L.; Tang, B. Z. *Macromol. Rapid Commun.* **2010**, *31*, 834−839.
(31) Bhalla, V.; Gupta, A.; Kumar, M. *Org. Lett.* **2012**, *14*, 3112−3115.
(32) Kumar, M.; Reja, S. I.; Bhalla, V. *Org. Lett.* **2012**, *14*, 6084−6087.
(33) Chandrasekhar, S. *Liq. Cryst.* **1993**, *14*, 3−14.
(34) Allen, M. T.; Diele, S.; Harris, K. M. D.; Hegmann, T.; Kariuki, M.; Lose, D.; Preece, J. A.; Tschierske, C. *J. Mater. Chem.* **2001**, *11*, 302−311.
(35) Raja, K. S.; Ramakrishnan, S.; Raghunathan, V. A. *Chem. Mater.* **1997**, *9*, 1630−1637.
(36) Kastler, M.; Pisula, W.; Wasserfallen, D.; Pakula, T.; Mullen, K. *J. Am. Chem. Soc.* **2005**, *127*, 4286−4296.
(37) Wu, J.; Baumgarten, M.; Debije, M. G.; Warman, J. M.; Mullen, K. *Angew. Chem., Int. Ed.* **2004**, *43*, 5331−5335.
(38) Zhi, L.; Mullen, K. *J. Mater. Chem.* **2008**, *18*, 1472−1484.
(39) Gross, M.; Muller, D. C.; Nothofer, H.-G.; Scherf, U.; Neher, D.; Brauchle, C.; Meerholz, K. *Nature* **2003**, *405*, 661−665.
(40) Dou, Xi.; Yang, X.; Bodwell, G. J.; Wagner, M.; Enkelmann, V.; Mullen, K. *Org. Lett.* **2007**, *9*, 2485−2488.
(41) Feng, X.; Pisula, W.; Takase, M.; Dou, X.; Enkelmann, V.; Wagner, M.; Ding, N.; Mullen, K. *Chem. Mater.* **2008**, *20*, 2872−2874.
(42) Jones, D. J.; Purushothaman, B.; Ji, S.; Holmes, A. B.; Wong, W. W. H. *Chem. Commun.* **2012**, *48*, 8066−8068.
(43) Wong, W. W. H.; Ma, C. Q.; Pisula, W.; Yan, C.; Feng, X.; Jones, D. J.; Mullen, K.; Janssen, R. A. J.; Bauerle, P.; Holmes, A. B. *Chem. Mater.* **2010**, *22*, 457−466.
(44) Wong, W. W. H.; Khoury, T.; Vak, D.; Yan, C.; Jones, D. J.; Crossley, M. J.; Holmes, A. B. *J. Mater. Chem.* **2010**, *20*, 7005−7014.
(45) Wong, W. W. H.; Subbiah, J.; Puniredd, S. R.; Purushothaman, B.; Pisula, W.; Kirby, N.; Mullen, K.; Jones, D. J.; Holmes, A. B. *J. Mater. Chem.* **2012**, *22*, 21131−21137.
(46) Wasserfallen, D.; Kastler, M.; Pisula, W.; Hofer, W. H.; Fogel, Y.; Wang, Z.; Mullen, K. *J. Am. Chem. Soc.* **2006**, *128*, 1334−1339.
(47) Terazono, Y.; Liddell, P. A.; Garg, V.; Kodis, G.; Brune, A.; Hambourger, M.; Moore, A. L.; Moore, T. A.; Gust, D. *J. Porphyrins Phthalocyanines* **2005**, *9*, 706−723.
(48) Bhalla, V.; Tejpal, R.; Kumar, M.; Puri, R. K.; Mahajan, R. K. *Tetrahedron Lett.* **2009**, *50*, 2649−2652.
(49) Tang, B. Z.; Geng, Y.; Lam, J. W. Y.; Li, B.; Jing, X.; Wang, X.; Wang, F.; Pakhomov, A.; Zhang, X. X. *Chem. Mater.* **1999**, *11*, 1581−1589.
(50) Demas, J. N.; Grosby, G. A. *J. Phys. Chem.* **1971**, *75*, 991−1024.
(51) Haidekker, M. A.; Theodorakis, E. A. *Org. Biomol. Chem.* **2007**, *5*, 1669−1678.
(52) Sohn, H.; Sailor, M. J.; Magde, D.; Trogler, W. C. *J. Am. Chem. Soc.* **2003**, *125*, 3821−3830.
(53) Vajpayee, V.; Kim, H.; Mishra, A.; Mukherjee, P. S.; Stang, P. J.; Lee, M. H.; Kim, H. K.; Chi, K.-W. *Dalton Trans.* **2011**, *40*, 3112.
(54) Albert, K. J.; Lewis, N. S.; Schauer, C. L.; Sotzing, G. A.; Stitzel, S. E.; Vaid, T. P.; Walt, D. R. *Chem. Rev.* **2000**, *100*, 2595−2626.
(55) Kim, T. H.; Lee, B. Y.; Jaworski, J.; Yokoyama, K.; Chung, W.-J.; Wang, E.; Hong, S.; Majumdar, A.; Lee, S.-W. *ACS Nano* **2011**, *5*, 2824−2830.